

## Article

# Microwave-Assisted Chemical Purification and Ultrasonication for Extraction of Nano-Fibrillated Cellulose from Potato Peel Waste

Mohsen Sadeghi-Shapourabadi <sup>1,2</sup> , Said Elkoun <sup>1,2,\*</sup>  and Mathieu Robert <sup>1,2</sup>

<sup>1</sup> Center for Innovation in Technological Ecodesign (CITE), University of Sherbrooke, Sherbrooke, QC J1K 2R1, Canada; mohsen.sadeghi.shapourabadi@usherbrooke.ca (M.S.-S.); mathieu.robert2@usherbrooke.ca (M.R.)

<sup>2</sup> Research Center for High Performance Polymer and Composite Systems (CREPEC), Montreal, QC H3A 0C3, Canada

\* Correspondence: said.elkoun@usherbrooke.ca

**Abstract:** Nanofibrillated cellulose was extracted from potato peel waste using a fast and green method with a simple process. To extract cellulose and eliminate non-cellulosic constituents, alkaline and hydrogen peroxide treatments were performed under microwave irradiation. The nanofibrillated cellulose was extracted from purified cellulose via TEMPO oxidation followed by ultrasonication. The TEM, FTIR, XRD, and TGA experiments were used to evaluate the structural, crystalline, and thermal properties of cellulose fiber and nanofiber. The chemical and FTIR analysis of bleached fibers indicates that almost all non-cellulosic components of biomass have been eliminated. The diameter of the extracted nanofibers is in the range of 4 to 22 nm. In terms of crystallinity, extracted nanocellulose had 70% crystallinity, compared to 17% for unprocessed lignocellulose fibers, which makes it an excellent choice for use as a reinforcement phase in biobased composites. Thermogravimetric analysis reveals that cellulose nanofibers are less thermally stable than potato peel pure cellulose, but it has a higher char content (28%) than pure cellulose (6%), which signifies that the carboxylate functionality acts as a flame retardant. The comparison between cellulose derived from microwave and conventional extraction methods confirmed that their impact on the removal of non-cellulosic materials is nearly identical, .

**Keywords:** potato peel waste; cellulose nanofibers (CNF); microwave assisted chemical treatment; TEMPO-oxidation; ultrasonic treatment



**Citation:** Sadeghi-Shapourabadi, M.; Elkoun, S.; Robert, M. Microwave-Assisted Chemical Purification and Ultrasonication for Extraction of Nano-Fibrillated Cellulose from Potato Peel Waste. *Macromol* **2023**, *3*, 766–781. <https://doi.org/10.3390/macromol3040044>

Academic Editors: Jungmok You and Jeonghun Kim

Received: 12 September 2023

Revised: 2 November 2023

Accepted: 12 November 2023

Published: 22 November 2023



**Copyright:** © 2023 by the authors. Licensee MDPI, Basel, Switzerland. This article is an open access article distributed under the terms and conditions of the Creative Commons Attribution (CC BY) license (<https://creativecommons.org/licenses/by/4.0/>).

## 1. Introduction

Recently, nanocellulose has gained considerable attention among researchers as a novel, abundant, and renewable material with high mechanical strength. This fact also can be due to the increasing interest of societies in utilizing biobased, degradable, and renewable materials.

Agricultural and food waste is mainly generated throughout numerous stages, including pre- and post-harvesting, storage, and rejections from industries, supermarkets, restaurants, and final consumers, which amounts to approximately 5.5 billion tons of annual global waste [1]. According to Fritsch, approximately 14,000 metric tons of potato pulp are produced solely in the European Union as a byproduct of starch manufacturing [2].

Potato, with the scientific name *Solanum tuberosum* L., is classified as a root vegetable and is the fourth most-produced agricultural product in the world after wheat, rice, and maize. Its global production was estimated at about 370 million tons per year in 2019. Potato waste is rich in starch, cellulose, hemicellulose, pectin, and proteins, which renders it a totally inexpensive, abundant, and renewable raw material for a variety of applications [3]. It is one of the major agro-waste generated by food and starch production

industries. To date, many value-added products have been derived from this waste material in an effort to alleviate the issue of excessive refuse production. The following are some examples of studies in this context. Production of a variety of value-added products, such as biocomposites and packaging materials [4–6], biofuel production [7], as well as the isolation of bioactive compounds, including phenolic compounds and alkaloids, which are widely used as antioxidants in the food industry [2,8,9]. In addition, thermoplastic starch products [10,11], starch nanocrystals [12,13], cellulose nanocrystals [14–16], and a multitude of other products are initiatives to reduce the generation of a substantial quantity of potato peel waste.

Cellulose is a natural polymer presenting in the cell wall of plants in form of bundles of rigid microfibrils surrounded with hemicellulose, lignin, or pectin [17,18]. The cellulose nanoparticles extracted from biomasses exhibit remarkable mechanical, optical, and barrier properties, while they are also fully renewable and biodegradable. Due to its exceptional properties, nanocellulose can be utilized in a variety of applications, including nanocomposites, coatings, environmentally friendly packaging materials, and biomedical applications, such as drug delivery vehicles, wound healing materials, and scaffolds for tissue engineering [19,20].

Cellulose nanoparticles are classified into two primary categories: cellulose nanofibrils (CNF) and cellulose nanocrystals (CNC). CNF and CNC have different shapes, sizes, and compositions. CNF are composed of bundles of cellulose chains and have a fibrous structure; they are typically several micrometers in length and 5–60 nanometers in width. The mechanical treatment of cellulose is a common method for disintegrating CNF. CNC, on the other hand, are rod-shaped and range in length from 100–500 nm and 5–20 nm in width. Typically, they are produced through the acid hydrolysis of cellulose fibers. In comparison to CNF, it exhibits higher thermal stability and crystallinity [21]. However, the mechanical procedures used to generate CNF are less harmful to the environment than the acid hydrolysis process used to produce CNC. Additionally, the production cost of CNF is generally lower than that of CNC [22]. Furthermore, CNF typically possesses several other benefits over CNC, including a higher surface area, improved flexibility, a higher aspect ratio, better alignment, and easier film-forming capability [21]. CNF has potential applications in different fields, including paper and packaging materials, composites, and biomedical applications. They are also utilized as a thickening agent in various formulations, such as paints, adhesives, and coatings [23].

In order to disintegrate cellulose nanofibrils from cellulose, there are multiple processes that can be utilized. One commonly used technique is mechanical disintegration, in which cellulose fibers are subjected to mechanical forces through processes such as grinding, refining, high-pressure homogenization, microfluidization, steam explosion, or sonication [24]. Another approach is the use of chemical pretreatments, such as TEMPO-mediated oxidation, as well as enzymatic hydrolysis that employs specific enzymes to degrade the amorphous regions of cellulose, leaving behind cellulose nanofibrils [25,26].

Thus far, several studies have been attempted on various potato waste materials with respect to the extraction of cellulose nanoparticles. Chen et al. investigated the potential of utilizing cellulose nanocrystals derived from potato peel waste in order to create biocomposites with enhanced mechanical and barrier characteristics. Initially, cellulose was purified through alkaline treatment (NaOH, 85 °C, 2.5 h, 3 times), then bleaching (Sodium Chlorite, 70 °C, 2 h, twice), and lastly, acidic hydrolysis was employed to produce CNC (H<sub>2</sub>SO<sub>4</sub>, 64%, 45 °C, 90 min). The extracted CNC showed an average fiber length of 410 nm with an aspect ratio of 41. They concluded that when compared to cotton-derived nanocellulose, cellulose extracted from potatoes resulted in substantially longer nanoparticles at comparable yields [16]. In 2019, Shruthy et al. dedicated their research to developing a PVA-based film incorporating cellulose nanoparticles as an alternative to standard packaging materials. The addition of cellulose nanoparticles to polyvinyl alcohol films enhanced their tensile strength, elongation, transparency, and thermal stability. The dimensions of the extracted nanoparticle are 50–100 nm in diameter and 100–200 nm in

length. In order to extract cellulose, alkaline treatment was employed, followed by alkaline bleaching, and finally, high-intensity acidic treatment was utilized to extract CNC [27]. In the other study published in 2023, Liu et al. optimized the preparation parameters of cellulose nanofibers derived from potato residues, which are the byproducts of a starch production facility. After the removal of starch using thermostable  $\alpha$ -amylase, the cellulose was purified using NaOH (7%, 70 °C, 1 h) and, lastly, H<sub>2</sub>O<sub>2</sub> solution (10%, 1.5 h, 70 °C). The nanofibrillation was accomplished by the use of ultrasonic waves, followed by a high-pressure homogenizer. They claimed the extracted nanofibers were 20–60 nm in diameter [28].

Interestingly, in recent years, researchers have been inclined towards employing more sustainable and less harmful methods for the extraction of cellulose. These processes have some mutual benefits, such as minimizing the use of chemicals or solvents, reducing processing time, and enhancing energy efficiency compared to conventional defibrillation methods. In this respect, more efficient and less energy-consuming techniques, such as microwave irradiation or ultrasonication treatments, have been utilized. In the study carried out by Imoolsup et al., microwave pretreatment in conjunction with high-shear and high-pressure homogenization was effectively used to improve the extraction of CNF from lime residue. They claimed that microwave pretreatment enhanced the production of nanofibrillated cellulose from lime while lowering energy consumption. It was proposed that the diameter of the obtained CNF was in the range of 3 to 46 nm, which was comparable to the diameter of CNF produced through chemical procedures [29].

The present study investigated the extraction of cellulose nanofiber from potato peel waste using a fast, chemically benign, and more sustainable approach by assisting microwave irradiation. For this purpose, in the initial step, cellulose purification is facilitated by the assistance of microwave irradiation throughout the chemical pretreatment process. Utilizing microwave irradiation shrinks the reaction time and enhances the efficiency of chemical pretreatment while consuming less energy than conventional heating methods. Furthermore, the subsequent nanofibrillation process is based on TEMPO oxidation, a chemically safe and environmentally benign reaction, and high-intensity ultrasonication, a green and energy-effective technique. In contrast, the previous attempts to produce cellulose nanoparticles from potato peel waste, including both CNF and CNC, employed the conventional heating approach to purify cellulose from biomass. To the best of the authors' knowledge, no study has been found on the extraction of cellulose nanofibers from potato peel waste using microwave irradiation [30–32].

The article is initially focused on the extraction of pure cellulose from potato peel waste by chemical treatment. After the separation of PW lignocellulose from its starch. The first step involved the alkaline treatment by a sodium hydroxide solution. The biomass was then bleached by alkaline hydrogen peroxide treatment, which resulted in the production of pure potato waste cellulose. All steps were performed once under microwave irradiation and once using a conventional heating apparatus for reference. The impact of chemical pretreatment on the removal of non-cellulosic substances was confirmed by Fourier-transform infrared spectroscopy (FTIR) and the chemical characterization of both methods. In the next stage, the cellulose nanofibers were extracted using the TEMPO oxidation, and then ultrasonication process. The extracted nanofibrillated cellulose was then characterized using various techniques, including transmission electron microscopy (TEM), Fourier-transform infrared spectroscopy (FTIR), X-ray diffraction (XRD), thermogravimetric analysis (TGA), and dispersion stability. These techniques were used to evaluate the structural, crystalline, thermal, and stability properties of cellulose nanofibers.

## 2. Materials and Methods

### 2.1. Materials

Two varieties of potatoes (yellow flesh and russet) were purchased at a local supermarket in Quebec for use in this investigation. The peels were separated from the flesh to extract cellulose and CNF from them. NaOH (98% purity), hydrogen peroxide (H<sub>2</sub>O<sub>2</sub>

30%), TEMPO 98% (2,2,6,6-Tetramethylpiperidine-1-yl)oxyl, sodium hypochlorite 96%, and sodium bromide, have been purchased from Sigma Aldrich, Oakville, Canada.

## 2.2. Extraction of Cellulose

The potatoes were first washed, peeled using a handy peeler, and dried for 24 h at 50 °C in a kitchen dryer. The dried PW was ground using a grinder with a mesh size of 40. The pulverized PW was subsequently heated with water (1:10 solid-to-liquid ratio) in a microwave chamber using an 1100-watt Panasonic microwave. The temperature of the mixture reached 100 °C due to the microwave radiation, and it was cooked for ten minutes. The cooked PW was then subjected to 10 min of high-speed homogenization at a rotation speed of 2000 rpm. To separate starch from lignocellulose, the cooked substance was thoroughly washed with an 85-micron metal sieve. The retained material was dried and stored for future chemical processes.

The chemical process used to extract cellulose was as follows: first, an alkaline treatment with Sodium Hydroxide (4% NaOH) was conducted twice, each time for 10 min (1:20 solid-to-liquid ratio). Then, in the second stage, the biomass was bleached with alkaline Hydrogen Peroxide (1% NaOH in combination with 7.5% H<sub>2</sub>O<sub>2</sub>) for 4 min with the solid-to-liquid ratio of 1:20. All treatments were carried out under microwave irradiation with a kitchen microwave on 1100 watt power. It is worth noting that after each treatment, the biomass was extensively washed to neutralize the residue and remove dissolved components.

To compare the effectiveness of microwave-assisted treatment versus conventional heating chemical treatment, the PW pulp was initially purified using the microwave technique and then with the conventional method (heater-stirrer) under similar treatment conditions; the only difference was the reaction time. The duration of the alkaline and bleaching steps in the microwave method was 10 and 4 min, respectively. In contrast, the conventional heating method required two hours for each step. The complete chemical process and defibrillation method are illustrated in Figure 1.

In addition, the yield amount was calculated based on the initial amount of dried potato peel waste. After each stage, the material was dried in an oven at 50 °C for 24 h, and the weight was measured. It was calculated with Equation (1):

$$\text{Yield \%} = M_C / M_{PW} \times 100 \quad (1)$$

where  $M_C$  was the weight of purified cellulose or CNF and  $M_{PW}$  was the weight of initial potato residue.

As depicted in Figure 1, the yield of purified cellulose was 7% for the microwave-assisted method and 6.3% for the conventional technique, respectively. The difference can be attributed to the length of the process since microwave-assisted treatment has less time to react, resulting in lower levels of biomass hydrolysis. After the nanofibrillation in the water, the CNF dispersion was centrifuged to precipitate any macrosized fibers. As a result, the yield of extracted nanofiber is somewhat lower, with 6.7% for the microwave technique as compared to 6.1% for the traditional approach.

## 2.3. Preparation of Cellulose

In order to nanofibrillate the PW cellulose, the TEMPO oxidation process was performed according to the method used by Isogai et al. and Saito et al. [33,34]. First of all, 2 g of extracted cellulose was dissolved in 200 milliliters of deionized water, followed by the addition of 0.2 g of Sodium Bromide (NaBr) and 0.04 g of TEMPO. The reaction was started by dropwise addition of 18 mL of Sodium Hypochlorite (12% concentration) to the solution. Throughout the reaction, the pH was maintained at  $10 \pm 0.2$  by adding a sodium hydroxide solution (0.5 M) until it no longer decreased. After 4 h, the reaction was considered complete, and, subsequently, it was quenched by adding 5 mL of ethanol and stirring for an additional 30 min. The resultant was washed with deionized water three times and dispersed in enough deionized water to have 0.5% *w/v* dispersion.

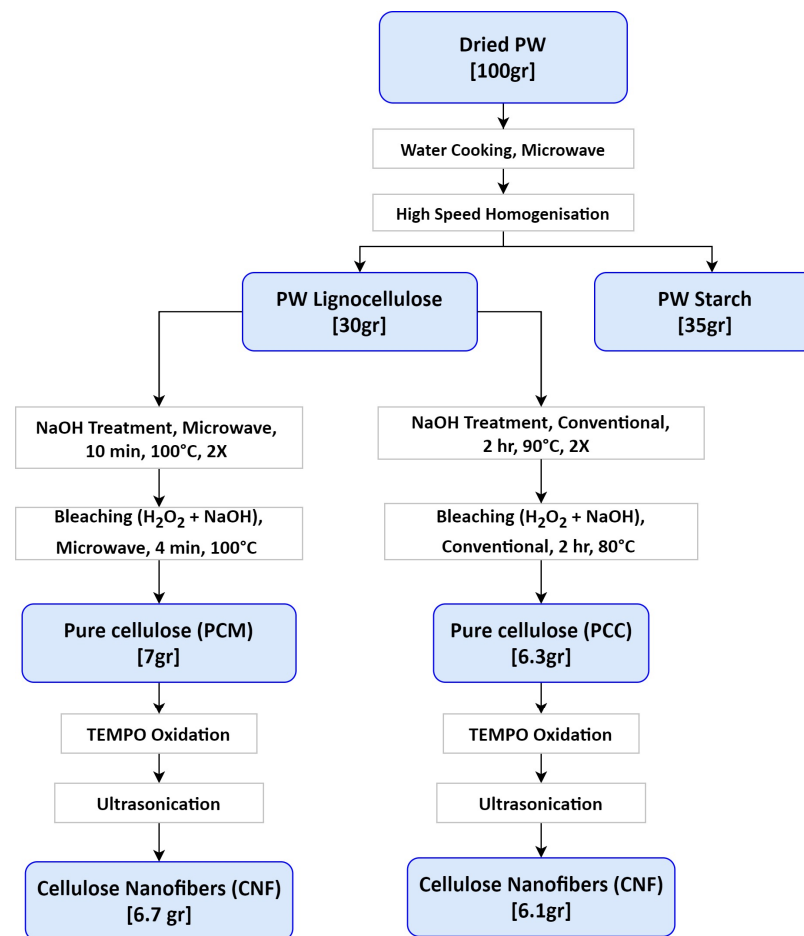


**Figure 1.** Detailed schematic overview of CNF preparation with each step's yield amount.

To achieve cellulose nanofibers, the TEMPO-oxidized cellulose (0.5% *w/v*), which was homogenized using a high-speed homogenizer, was subjected to ultrasonic treatment using a Qsonic Q700 ultrasonic machine, Cole-Parmer, Quebec, Canada, equipped with a cylindrical titanium alloy probe operating at a frequency of 20 kHz. The ultrasonic treatment was carried out for 30 min at an amplitude of 80. Throughout the treatment, the container was placed in an ice bath in order to prevent heat production and fiber damage. Subsequently, the resulting nanofibers were stored in a refrigerator for further experiments.

## 2.4. Characterization

### 2.4.1. Chemical Characterization

The chemical composition of fibers before and after the chemical treatment was assessed using a modified van Soest method. To be specific, the ANKOM A200 (Ankom, Macedon, NY, USA) Filter Bag Technique (FBT) was employed for conducting this assessment [29,30]. In order to perform this test, first, the solid samples were screened to have a uniform particle size (20–65 mesh) and then dried at 105 °C for 24 h prior to analysis to have a dryness of more than 95%. Using this procedure, the contents of cellulose, lignin, hemicellulose, and extractives were measured. The percentages of the mentioned components were calculated from the difference between neutral detergent fiber (NDF), acid detergent fiber (ADF), and acid detergent liquid (ADL), as indicated following [31]:

$$\begin{aligned}
 \text{Extractives (\%)} &= 100\% - \text{NDF (\%)} \\
 \text{Hemicellulose (\%)} &= \text{NDF (\%)} - \text{ADF (\%)} \\
 \text{Cellulose (\%)} &= \text{ADF (\%)} - \text{ADL (\%)} \\
 \text{Lignin (\%)} &= \text{ADL (\%)}
 \end{aligned}
 \tag{2}$$

#### 2.4.2. FTIR

Fourier-transform infrared spectroscopy (FTIR) spectra were measured by a JASCO 4600 spectrometer (Japan) equipped with an ATR PRO ONE reflection accessory. Spectra were obtained with a resolution of  $4\text{ cm}^{-1}$  and in the range  $4000\text{--}600\text{ cm}^{-1}$ . FTIR was performed on unprocessed, alkaline-treated (PL-A), bleached, and oxidized cellulose, as well as cellulose nanofibers, to understand the functional groups present in each sample. The samples were ground into fine powder using a ball mill and subjected to analysis.

#### 2.4.3. XRD

The PANalytical X-Pert Pro MPD diffractometer was utilized to obtain the crystalline structure of raw PW lignocellulose, pure cellulose, and dried PCNF, which were pulverized using a ball miller. The apparatus is outfitted with a general area detector diffraction system that utilizes Copper  $K\alpha$  radiation ( $\lambda = 1.542\text{ \AA}$ ). The system has a  $2\theta$  (Braggs angle) range spanning from  $5^\circ$  to  $40^\circ$ , with a step size of  $0.04$ . The Segal et al. method's empirical equation was utilized to compute the crystallinity index (CrI) of the structure [32].

$$CrI = (I_{002} - I_{am}) / I_{002} \quad (3)$$

where,  $I_{am}$  is the XRD intensity taken at  $2\theta = 18^\circ$  as the characteristic pattern of the amorphous part of cellulose, and  $I_{002}$  is the intensity of diffraction peak at  $2\theta = 22.6^\circ$  which is correlated by the crystalline region of cellulose [33,34].

#### 2.4.4. Transmission Electron Microscopy (TEM)

Transmission electron microscopy was used in order to examine the morphology, size, and fibrillation extent of the PW nanocellulose. To achieve this, the extracted nanocellulose was prepared with a solid content of  $0.1\text{ wt}\%$ , sonicated for  $10\text{ min}$ , and subsequently cast on glow-discharged carbon-coated TEM grids (300-mesh copper Formvar/carbon-coated grids). Then, the samples were dried by filter paper absorption. To enhance resolution, the dried samples were stained with a  $2\text{ wt}\%$  solution of uranyl acetate, followed by drying the excess solution with filter paper. The characterization was performed using a transmission electron microscope (Hitachi H7500) operated at a  $100\text{ kV}$  accelerating voltage.

#### 2.4.5. TGA

Thermogravimetric analysis was conducted to evaluate the thermal stability of the raw lignocellulose, PWC, as well as the oxidized and extracted cellulose nanofiber. The TGA4000–Perkin Elmer instrument was employed to measure the weight loss as a function of the temperature in the range of  $30\text{--}650\text{ }^\circ\text{C}$ . The heating rate was  $10\text{ }^\circ\text{C min}^{-1}$ , and the experiment was performed under a nitrogen atmosphere.

#### 2.4.6. Dispersion Stability

The assessment of suspension stability was carried out on three different materials, namely PCM, oxidized cellulose, and PCNF. To accomplish this, each sample was dispersed in water using ultrasonication for  $10\text{ min}$ . The visual appearance of the samples was assessed at specified intervals to determine any changes.

### 3. Results and Discussion

#### 3.1. Confirmation of Removal of Lignin and Hemicellulose

##### 3.1.1. Fiber Chemical Analysis

FBT Chemical analysis is a technique for determining the quantity of cellulose, hemicellulose, lignin, and extractible in the structure of a lignocellulosic material, which is used to admit the removal of non-cellulosic substances [35].

As revealed by Table 1, the chemical composition of unprocessed biomass (PL) was approximately  $32\%$  cellulose,  $42\%$  hemicellulose, and  $19\%$  lignin, according to results from FBT analysis. It can be claimed that both microwave and conventional chemical treatments omit a significant amount of hemicellulose and lignin from the structure. More precisely,

hemicellulose was removed by 90% and 88%, and lignin was eliminated by 97% and 92% by the conventional and microwave techniques, respectively. Accordingly, the content of cellulose increased from approximately 32% in PL to 87% and 84% by conventional and microwave methods, respectively. It can also be said that the impact of microwave and conventional treatment to remove the non-cellulosic materials is quite similar. In every instance, more than 88% of non-cellulosic constituents were eliminated. However, the removal in the former method is slightly higher than the latter one, which can be due to the fact that in the conventional method, there has been more hydrolysis time to eliminate non-cellulosic materials [36].

**Table 1.** Chemical characterization of raw PW lignocellulose (PL), cellulose extracted by microwave (PCM), cellulose extracted by conventional (PCC) method.

	Cellulose	Hemicellulose	Lignin	Extractible
PL (Raw)	32.27 ± 0.3	42.23 ± 1.7	19.08 ± 0.34	5.12 ± 1.6
PCC	87.36 ± 0.36	4.09 ± 0.22	0.43 ± 0.22	6.67 ± 0.2
PCM	84.44 ± 0.77	5.2 ± 0.61	1.48 ± 0.27	7.13 ± 0.69

Other studies have been conducted to examine the influence of microwave on chemical pretreatment. Harini et al. extracted cellulose nanofibers from the banana peel and bract by assisting microwave. The microwave was only in the first step, cooking with water to eliminate the impurities from cellulose. It was claimed that the microwave digestion process was excellent for producing cellulose microfibrils. The extraction yield of micro-cellulose fiber from residual banana peel and bract was determined to be 55% and 65%, respectively [37]. In 2016, Chowdhury et al. extracted cellulose nanocrystals from jute stalk using ultrasonication combined with microwave-assisted pretreatment. The dried jute stalk powder was pretreated using sodium hydroxide under microwave irradiation, which caused the partial delignification of jute stalk samples. After preliminary alkaline treatment, the yield was reported to be 65%, with hemicellulose and lignin reduced by 36% and 82%, respectively [38].

Regarding the yield amount, as depicted in Figure 1, the yield of purified cellulose was 7% for the microwave-assisted method and 6.3% for the conventional technique, respectively. The difference can be attributed to the length of the process since microwave-assisted treatment has less time to react, resulting in lower levels of biomass hydrolysis. After the nanofibrillation in the water, the CNF dispersion was centrifuged to precipitate any macrosized fibers. As a result, the yield of extracted nanofiber is somewhat lower, with 6.7% for the microwave technique as compared to 6.1% for the traditional approach.

However, there are other studies with higher yields than the current study, such as Liu's research, which had a yield of 19.8%. The reason can stem from the difference in resource materials. The potato waste utilized in their research originated from a starch production facility, which resulted in the maximum amount of starch removal in the manufacturing process. Whereas, in the current study, the potato peel waste contains a significant amount of starch that was not removed beforehand [28].

In general, by opening up the compact structure of biomass, microwaves enable chemicals to penetrate more easily into the structure and accelerate the hydrolysis of hemicellulose and lignin. Compared to the conventional method, this approach offers several benefits, such as reduced reaction time, decreased energy consumption, lower costs, and improved environmental sustainability. All of the aforementioned benefits, along with similar purification outcomes, make microwave irradiation a competent alternative for the chemical purification of cellulose in potato peel waste biomass. However, with regard to energy consumption, the power consumption of the heater stirrer was recorded at 2000 watts, while the microwave consumed 1100 watts. Taking into account the reaction time, it can be estimated that the microwave treatment consumes 80% less power than the conventional chemical treatment.

### 3.1.2. FTIR Spectroscopy

The FTIR test was conducted to assess the presence of lignin, hemicellulose, and pectin, as well as to examine changes that occurred at different stages in the chemical procedure (alkaline, bleaching, and oxidizing); the findings are presented in Figure 2.

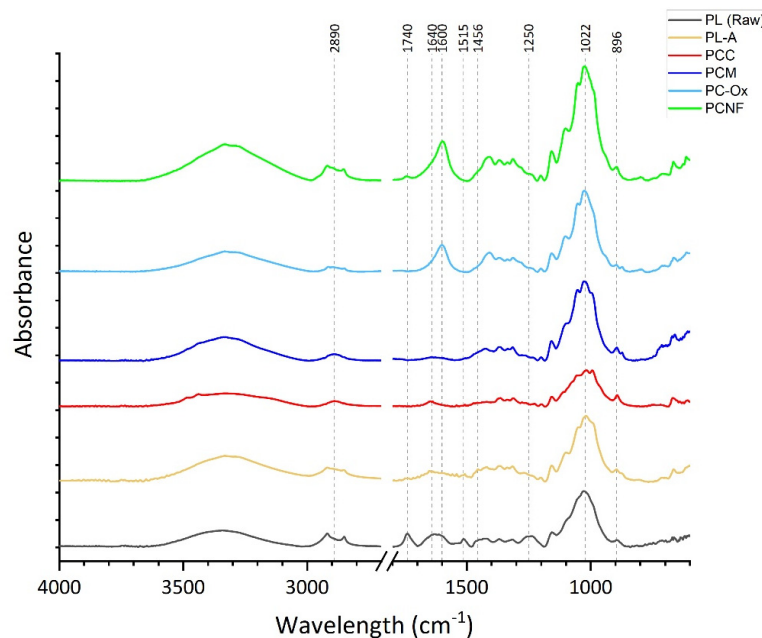


**Figure 2.** FTIR peaks for raw lignocellulose (PL Raw), after alkaline (PL–A), conventional purified cellulose (PCC), microwave purified cellulose (PCM), TEMPO–oxidised cellulose (PC–Ox), and CNF from potato peel waste (PCNF).

The FTIR spectra of cellulose, hemicellulose, and lignin exhibit two prominent and robust absorption peaks. The spectral feature observed between the wavenumber range of 3000 to 3500  $\text{cm}^{-1}$  is commonly associated with the OH stretching vibrations, which can be attributed to the presence of intermolecular hydrogen bonding within the materials [39,40]. Another peak near 2890  $\text{cm}^{-1}$  is related to the asymmetric and symmetric stretching vibrations of  $\text{CH}_2$  [41,42]. Clearly, these major peaks are present in all FTIR-analyzed samples.

There are two characteristic peaks in hemicellulose, one at 1740  $\text{cm}^{-1}$  and another at 1250  $\text{cm}^{-1}$ , which are attributed to hemicellulose's carboxylic acid and ester groups [43,44]. The disappearance of both spectra following alkaline treatment demonstrates that hemicellulose was removed using the sodium hydroxide solution [36,45].

Additionally, the bleaching procedure eliminates lignin to a significant degree. It is supported by the disappearance of peaks 1456 and 1515  $\text{cm}^{-1}$ , which correspond to  $\text{C}=\text{C}$  vibrations in lignin's aromatic skeleton, and the 1640  $\text{cm}^{-1}$  bond corresponding to  $\text{C}=\text{O}$  vibrations originating from lignin's carbonyl groups [42].

Regarding cellulose, the region between 800 and 1500  $\text{cm}^{-1}$  is a unique fingerprint region in which a majority of characteristic bonds remained unchanged. This indicates that regardless of alkali or bleaching treatment the cellulose maintains its chemical structure to the original untreated one [40,46].

The characteristic band of TEMPO-oxidized cellulose has a peak at 1600  $\text{cm}^{-1}$ , which reveals the presence of a carboxylated group and confirms the oxidation of cellulose by TEMPO. Furthermore, there was no significant difference found between the spectra of the oxidized biomass and the nanofibers, demonstrating that the nanofibrillation process using ultrasonic irradiation did not alter the chemical structures of the oxidized fibers [36].

### 3.2. Structural Morphology

#### Morphological Observation of CNF (TEM)

TEM microscopy was employed to examine the size and structural morphology of the extracted nanofibers. The resulting TEM images of PCNF at a  $25,000\times$  magnification are depicted in Figure 3a,b, confirming the presence of individual nanofibers. It can be argued that the forces introduced by the collapse of cavitation bubbles created by ultrasonic waves were strong enough to defibrillate the cellulose fibers. Also to be considered is the effect of sonication waves on the dissociation of hydrogen bonds. As a result of the mentioned influences, the fibers were completely disintegrated, and a network of interconnected nanofibers was formed [47,48].

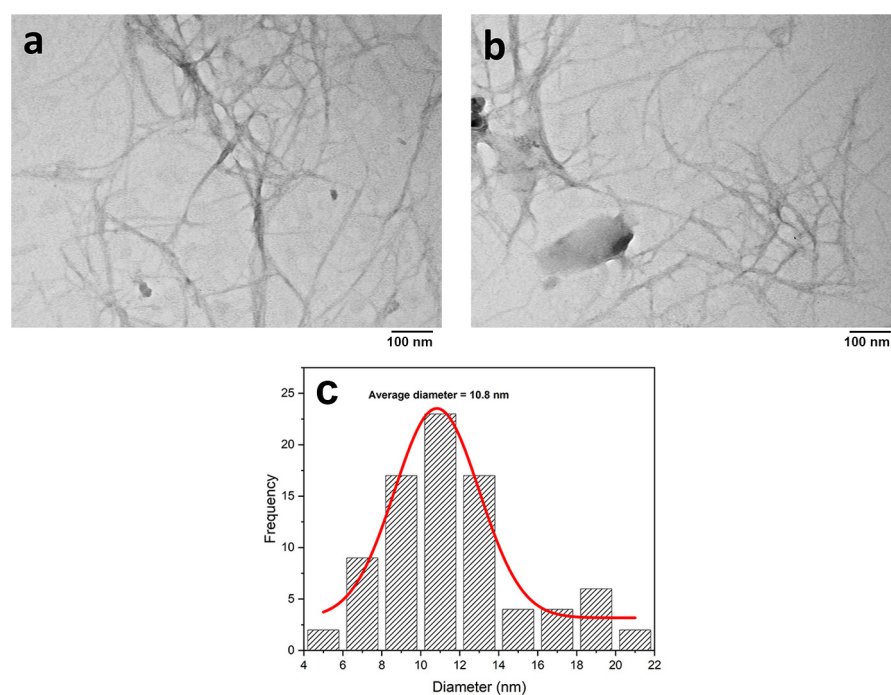


**Figure 3.** (a,b) TEM images of potato peel CNF. (c) Nanofiber's diameter distribution.

The TEM images and the diameter distribution statistics revealed that the aqueous suspension contained a large number of nanometer-scale fibers and some fibril bundles. The diameter of the extracted nanofibers was determined by processing the TEM images using ImageJ analysis software (version 1.52). The diameter of distinct nanofibers ranges from 4 to 22 nanometers, with an average diameter of 10.8 nm, as shown in Figure 3c. Figure 3c also represents the diameter distribution of the nanofibers. Notably, about 68% of fibers had a diameter between 8 and 14 nm, 13% of the fibers had a diameter within 4–8 nm, while only 20% of the fibers had a diameter greater than 14 nm.

For comparison, the diameter of the nanofibers obtained in this investigation was comparable to that of cellulose nanofibers isolated from citrus residue and sugarcane bagasse in other studies. In these studies, the diameters for nanofibers prepared by using enzymatic and chemo-mechanical processes were around 7–13 nm and 10–20 nm, respectively [46,47]. The results are also comparable to those reported by Liu et al. According to their findings, the diameter of TEMPO-oxidized CNF ranges from 10 to 50 nanometers. It has been mentioned that the diameter of TEMPO-oxidized fibers is smaller than the nanofibers extracted mechanically from potato residues using high-shear grinders. This difference can be attributed to the accelerated degradation process of cellulose enabled by TEMPO oxidation [28].

### 3.3. Crystalline Properties (XRD)

The X-ray diffraction (XRD) technique was employed to investigate the crystallinity degree of the potato peel fibers at each stage. The XRD patterns of the unprocessed biomass, pure and oxidized cellulose, as well as the extracted CNF, are illustrated in Figure 4. As shown in the graph, the diffraction pattern of all samples exhibited similar characteristic peaks at around  $2\theta = 16.5^\circ$ ,  $2\theta = 22.5^\circ$ , and another peak at approximately  $30^\circ$  [36,49]. Among the aforementioned peaks, the  $16.5^\circ$  and  $22.5^\circ$  correspond to the (1 1 0) and (2 0 0) crystallographic planes of cellulose I, respectively. The intensity of  $18^\circ$  also represents the contribution of the amorphous fraction in the cellulose I structure [40,42,50]. The results indicate that both microwave and conventional extraction methods provide cellulose with similar crystalline structures.

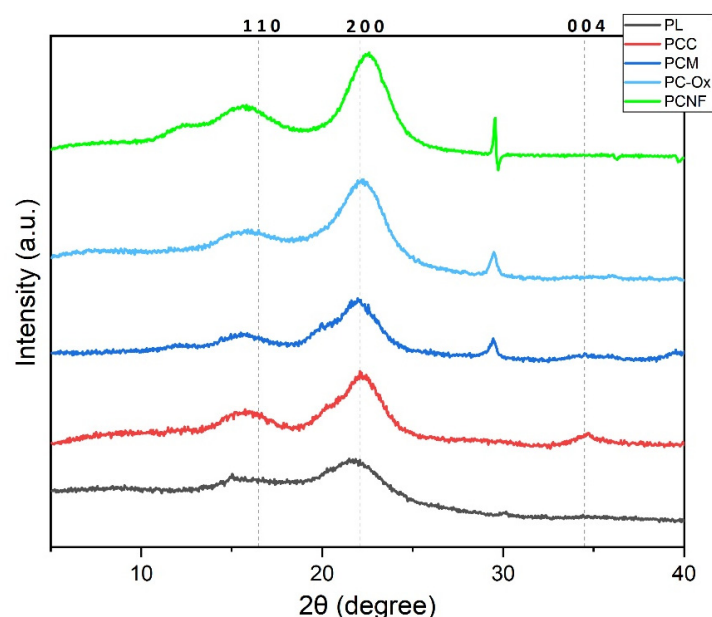


**Figure 4.** XRD spectra of raw lignocellulose (PL), conventional purified cellulose (PCC), microwave purified cellulose (PCM), TEMPO-oxidized cellulose (PC-Ox), and cellulose nanofibers (PCNF) from potato peel waste.

The crystallinity index (CrI) is a useful factor for comparing the fractions of amorphous and crystalline components in the sample, as calculated by the Segal equation. The CrI of the raw biomass resulted in a value of 17%, while the value for the pure cellulose increased to 52%. The observed phenomenon is attributed to the elimination of amorphous lignin, hemicellulose, and extractive fractions from the structure [46,51]. Liu et al. have also reported the CrI for raw potato waste and pure cellulose from potato residue, by 11.26% and 53%, respectively, which are comparable to current results and support the use of microwaves during chemical treatment [28]. In addition, by removing non-crystalline components, the hydroxyl groups of cellulosic chains formed intramolecular and intermolecular hydrogen bonds. This bonding impeded the free movement of cellulosic chains and forced them to form an orientation, resulting in an increase in crystallinity [45].

The characteristic peaks and crystallinity index of cellulose extracted by the conventional method are similar to those extracted by microwave (55% and 52%, respectively). This justifies the use of microwaves rather than conventional heating in the chemical treatment stages required to purify cellulose, as both methods produce nearly identical results. It is also supported by the FTIR results provided in its section.

The characteristic peaks of pure PCM and oxidized cellulose exhibit no noticeable changes. However, the crystallinity index of oxidized cellulose exhibited a slightly lower intensity (46% for oxidized as compared to PCM with 52%), which implies that the process of oxidation did not significantly alter the crystalline structure of cellulose [36]. The minor

decrease after the oxidation process could be attributed to the disruption of hydrogen bonds, which results in the formation of certain amorphous regions [47].

The defibrillation of fibers by ultrasonic waves results in the destruction of inter-fibril bonds and the formation of nano-sized fibers with large surface areas. This resulted in a rise in the number of hydrogen bonds between accessible –OH groups of the fibrillated fibers, which caused the crystallinity index to increase to 70% [48]. Interestingly, the values are consistent with the CrI estimated for TEMPO-oxidized CNF published by Liu et al., which was 64.3% [28].

#### 3.4. Thermal Properties of Nanofibers (TGA)

The thermogravimetric analysis was used to characterize the thermal behavior of unprocessed and chemically and mechanically treated potato peel fibers. Figure 5a depicts the results for weight loss as a function of temperature, while Figure 5b depicts the corresponding DTG curves. The peaks observed on the DTG curves represented the maximal degradation rate temperature (Tmax), which was associated with the thermal decomposition of each material. It is important to note that more stable substances are those that can withstand higher temperatures without experiencing weight loss.

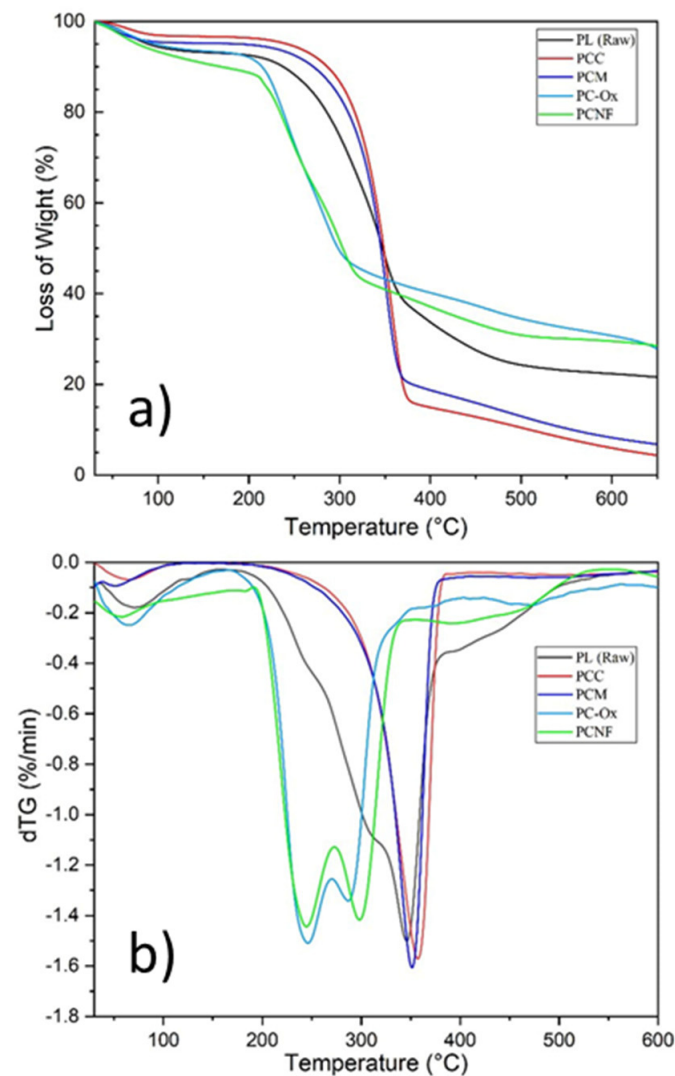


**Figure 5.** (a) Thermogravimetric graph, (b) DTG graph: raw lignocellulose (PL), conventional purified cellulose (PCC), microwave purified cellulose (PCM), TEMPO–oxidized Cellulose (PC–Ox), and cellulose nanofibers (PCNF) from potato peel waste.

Regardless of the sample, there is an initial weight loss observed under the temperature of 100 °C, which is owing to the evaporation of the moisture absorbed to the biomass [52,53]. With respect to pure cellulose, it has been observed that its decomposition (T<sub>max</sub>) initiates at approximately 345 °C. According to Pacaphol, the reason for the high thermal stability of pure cellulose is attributed to its composition, which consists of long linear polymer chains of β-glucose without branches [54]. In comparison, the raw biomass (PL) exhibits a prominent peak at 345 °C, which corresponds to the degradation of cellulose, and a minor shoulder around 300 °C that is attributed to the presence of impurities, such as lignin and hemicelluloses [43]. The absence of the shoulder in the purified cellulose suggests that the NaOH and H<sub>2</sub>O<sub>2</sub> chemical treatment was successful in eliminating non-cellulosic components.

Whereas the thermal degradation of pure cellulose is around 345 °C, for the TEMPO-oxidized cellulose and the cellulose nanofiber, it happened at 245 °C. This significant decrease can be due to lower thermal degradation of carboxylate anions (COO<sup>-</sup>) on the C6 carbon of cellulose chain [34,55]. It can also be claimed that the reduction in cellulose crystallinity, resulting from its oxidation, is another contributing factor to the decrease in degradation temperature, as corroborated by the CrI in the XRD analysis [56].

The residual char after 600 °C can be used to determine the presence of hemicellulose, lignin, and ash content. In the case of pure cellulose, the residual char is 6%, while in raw biomass, it is comparatively higher and is around 21%. The existence of lignin in the raw biomass can be one factor in this phenomenon. In other words, the pyrolysis of lignin generates more residual char than cellulose [44]. In comparison, the TEMPO-oxidized cellulose and cellulose nanofibers have much higher residual char compared to the bleached cellulose, with 26% and 28%, respectively. This phenomenon can be attributed to the incorporation of carboxylate functionalities produced by the TEMPO oxidation process. In fact, the introduction of carboxylate groups had a flame-retardant effect, resulting in a higher amount of residue left after heating [56].

In the research conducted by Liu et al., cellulose was extracted from potato residue without subjecting it to microwave treatment. The outcomes are nearly identical. Their findings revealed that thermal degradation of pure cellulose occurs at 337 °C, whereas it occurs at 345 °C in the microwave-assisted method. This indicates that the microwave procedure has no detrimental influence on the thermal stability of potato-based cellulose. Furthermore, they claimed that the T<sub>max</sub> for their potato-based nanofiber extracted by grinding technique was 337 °C, which is much higher than the T<sub>max</sub> for CNF extracted in this article, which was 245 °C. However, they determined the T<sub>max</sub> for TEMPO-oxidized CNF to be 270 °C, which is roughly similar to the value reported in this study [28].

### 3.5. Dispersion Stability

The stability for water dispersion of PW-Cellulose, oxidized cellulose and final nanocellulose over specified sedimentation times is depicted in Figure 6. It was evident from the results that the stability of pure cellulose is notably inferior to that of oxidized cellulose and PCNF, as demonstrated by the sedimentation process, which took approximately 2 h for pure PCM (Figure 6B). Compared to pure cellulose, oxidized cellulose displayed higher stability, even after 24 h (Figure 6D). Finally, the CNF exhibited complete stability without any precipitation within the 24 h time frame (Figure 6F). Thus, it can be concluded that the primary factor responsible for the dispersion is the charge difference between PCNF and pure cellulose (PCM), which can be attributed to the negative charge of carboxylate anions substituted on the cellulose chains during the TEMPO oxidation process [57]. These negatively charged groups cause the repulsion force and prevent the particles from aggregating and precipitation [56].

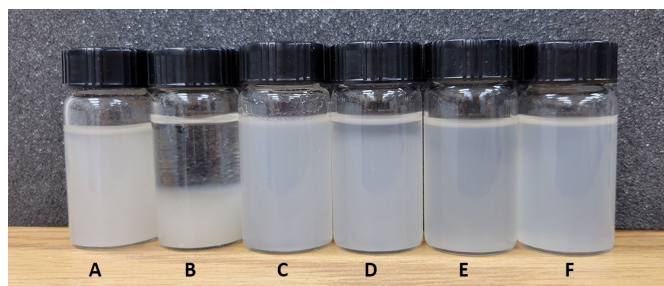


**Figure 6.** Precipitation in the samples of (A) PCM (immediately), (B) PCM (after 2 h), (C) Oxidized-PC (immediately), (D) Oxidized-PC (after 24 h), (E) PCNF (immediately), (F) PCNF (after 24 h).

#### 4. Conclusions and Future Scope

This investigation aims to valorize potato peel waste as an inexpensive waste resource without the need for excessive energy consumption or the use of intense and harmful chemicals. In this investigation, cellulose nanofibers were extracted from potato peel residue using a simple, eco-friendly, and efficient procedure. In the first stage, chemical purification (NaOH and then bleaching with  $H_2O_2$ ) is performed under microwave irradiation, and in the second step, cellulose nanofiber is extracted by TEMPO oxidation followed by ultrasonication. TEM analysis revealed that the diameter of cellulose nanofibers derived from potato peel waste ranged between 4 and 22 nanometers. Analyzing the XRD graph, it was determined that the extracted nanofibers' crystalline properties were 70%, which is a significant increase from the 17% of the unprocessed material. By comparing the cellulose extracted by microwave irradiation and the conventional heating method, it can be concluded that the microwave provides cellulose fibers with nearly the same properties as the conventional heating method while reducing the reaction time from two hours to less than 10 min and the amount of energy consumption by 80%.

Despite the promising results observed in laboratory settings, it would be beneficial to identify the potential solutions to enable the implementation of this method on a larger scale and in mass production. Additional research is also required to optimize the extraction conditions in order to increase the yield and quality of nano-fibrillated cellulose.

**Author Contributions:** Conceptualization, M.S.-S., S.E. and M.R.; validation, S.E., M.R. and M.S.-S.; investigation, M.S.-S.; writing—original draft preparation, M.S.-S.; writing—review and editing, M.S.-S., S.E. and M.R.; visualization, M.S.-S.; supervision, S.E. and M.R. All authors have read and agreed to the published version of the manuscript.

**Funding:** This research received no external funding.

**Institutional Review Board Statement:** Not applicable.

**Informed Consent Statement:** Not applicable.

**Data Availability Statement:** The data presented in this study are available on request from the corresponding author.

**Acknowledgments:** The authors want to thank “Natural Sciences and Engineering Research Council” of Canada (NSERC) and Centre de Recherche sur les Systèmes Polymères et Composites (CREPEC).

**Conflicts of Interest:** The authors declare no conflict of interest.

#### Abbreviations

PW	Potato peel waste
PL	Potato peel lignocellulose
PCC	Potato peel cellulose-conventional extracted method
PCM	Potato peel cellulose-microwave extracted method
PC-Ox	Potato peel TEMPO-oxidized cellulose

PCNF	Potato peel cellulose nanofibers
CNF	Cellulose nanofibers
CNC	Cellulose nanocrystals
FTIR	Fourier-transform infrared spectroscopy
XRD	X-ray diffraction
TGA	Thermogravimetric analysis
TEM	Transmission electron microscopy

## References

- Cherubin, M.R.; Oliveira, D.M.d.S.; Feigl, B.J.; Pimentel, L.G.; Lisboa, I.P.; Gmach, M.R.; Varanda, L.L.; Morais, M.C.; Satiro, L.S.; Popin, G.V. Crop residue harvest for bioenergy production and its implications on soil functioning and plant growth: A review. *Sci. Agric.* **2018**, *75*, 255–272. [\[CrossRef\]](#)
- Fritsch, C.; Staebler, A.; Happel, A.; Cubero Márquez, M.A.; Aguiló-Aguayo, I.; Abadias, M.; Gallur, M.; Cigognini, I.M.; Montanari, A.; López, M.J. Processing, valorization and application of bio-waste derived compounds from potato, tomato, olive and cereals: A review. *Sustainability* **2017**, *9*, 1492. [\[CrossRef\]](#)
- Ncobela, C.N.; Kanengoni, A.T.; Hlatini, V.A.; Thomas, R.S.; Chimonyo, M. A review of the utility of potato by-products as a feed resource for smallholder pig production. *Anim. Feed Sci. Technol.* **2017**, *227*, 107–117. [\[CrossRef\]](#)
- Sepelev, I.; Galoburda, R. Industrial potato peel waste application in food production: A review. *Res. Rural Dev.* **2015**, *1*, 130–136.
- Xie, Y.; Niu, X.; Yang, J.; Fan, R.; Shi, J.; Ullah, N.; Feng, X.; Chen, L. Active biodegradable films based on the whole potato peel incorporated with bacterial cellulose and curcumin. *Int. J. Biol. Macromol.* **2020**, *150*, 480–491. [\[CrossRef\]](#)
- Othman, S.H.; Edwal, S.A.M.; Risyon, N.P.; Basha, R.K.; A TALIB, R. Water sorption and water permeability properties of edible film made from potato peel waste. *Food Sci. Technol.* **2017**, *37*, 63–70. [\[CrossRef\]](#)
- Liang, S.; McDonald, A.G. Anaerobic digestion of pre-fermented potato peel wastes for methane production. *Waste Manag.* **2015**, *46*, 197–200. [\[CrossRef\]](#)
- Martinez-Fernandez, J.S.; Seker, A.; Davaritouchaee, M.; Gu, X.; Chen, S. Recovering valuable bioactive compounds from potato peels with sequential hydrothermal extraction. *Waste Biomass Valorization* **2021**, *12*, 1465–1481. [\[CrossRef\]](#)
- Al-Weshahy, A.; Rao, A.V. Isolation and characterization of functional components from peel samples of six potatoes varieties growing in Ontario. *Food Res. Int.* **2009**, *42*, 1062–1066. [\[CrossRef\]](#)
- Islam, H.B.M.Z.; Susan, M.A.B.H.; Imran, A.B. Effects of plasticizers and clays on the physical, chemical, mechanical, thermal, and morphological properties of potato starch-based nanocomposite films. *ACS Omega* **2020**, *5*, 17543–17552. [\[CrossRef\]](#)
- Talja, R.A.; Helén, H.; Roos, Y.H.; Jouppila, K. Effect of various polyols and polyol contents on physical and mechanical properties of potato starch-based films. *Carbohydr. Polym.* **2007**, *67*, 288–295. [\[CrossRef\]](#)
- Gujral, H.; Sinhmar, A.; Nehra, M.; Nain, V.; Thory, R.; Pathera, A.K.; Chavan, P. Synthesis, characterization, and utilization of potato starch nanoparticles as a filler in nanocomposite films. *Int. J. Biol. Macromol.* **2021**, *186*, 155–162. [\[CrossRef\]](#) [\[PubMed\]](#)
- Hasanin, M.S. Simple, economic, ecofriendly method to extract starch nanoparticles from potato peel waste for biological applications. *Starch-Stärke* **2021**, *73*, 2100055. [\[CrossRef\]](#)
- Raigond, P.; Raigond, B.; Kochhar, T.; Sood, A.; Singh, B. Conversion of Potato Starch and Peel Waste to High Value Nanocrystals. *Potato Res.* **2018**, *61*, 341–351. [\[CrossRef\]](#)
- Olad, A.; Doustdar, F.; Gharekhani, H. Fabrication and characterization of a starch-based superabsorbent hydrogel composite reinforced with cellulose nanocrystals from potato peel waste. *Colloids Surf. A Physicochem. Eng. Asp.* **2020**, *601*, 124962. [\[CrossRef\]](#)
- Chen, D.; Lawton, D.; Thompson, M.R.; Liu, Q. Biocomposites reinforced with cellulose nanocrystals derived from potato peel waste. *Carbohydr. Polym.* **2012**, *90*, 709–716. [\[CrossRef\]](#)
- Bruce, D.; Hobson, R.; Farrent, J.; Hepworth, D. High-performance composites from low-cost plant primary cell walls. *Compos. Part A Appl. Sci. Manuf.* **2005**, *36*, 1486–1493. [\[CrossRef\]](#)
- Heidarian, P.; Behzad, T.; Sadeghi, M. Investigation of cross-linked PVA/starch biocomposites reinforced by cellulose nanofibrils isolated from aspen wood sawdust. *Cellulose* **2017**, *24*, 3323–3339. [\[CrossRef\]](#)
- Shaghaleh, H.; Xu, X.; Wang, S. Current progress in production of biopolymeric materials based on cellulose, cellulose nanofibers, and cellulose derivatives. *RSC Adv.* **2018**, *8*, 825–842. [\[CrossRef\]](#)
- Moon, R.J.; Martini, A.; Nairn, J.; Simonsen, J.; Youngblood, J. Cellulose nanomaterials review: Structure, properties and nanocomposites. *Chem. Soc. Rev.* **2011**, *40*, 3941–3994. [\[CrossRef\]](#)
- Trache, D.; Tarchoun, A.F.; Derradji, M.; Hamidon, T.S.; Masruchin, N.; Brosse, N.; Hussin, M.H. Nanocellulose: From fundamentals to advanced applications. *Front. Chem.* **2020**, *8*, 392. [\[CrossRef\]](#)
- Xu, X.; Liu, F.; Jiang, L.; Zhu, J.; Haagenson, D.; Wiesenborn, D.P. Cellulose nanocrystals vs. cellulose nanofibrils: A comparative study on their microstructures and effects as polymer reinforcing agents. *ACS Appl. Mater. Interfaces* **2013**, *5*, 2999–3009. [\[CrossRef\]](#)
- Zeng, J.; Zeng, Z.; Cheng, Z.; Wang, Y.; Wang, X.; Wang, B.; Gao, W. Cellulose nanofibrils manufactured by various methods with application as paper strength additives. *Sci. Rep.* **2021**, *11*, 11918. [\[CrossRef\]](#)
- Kaur, P.; Sharma, N.; Munagala, M.; Rajkhowa, R.; Aallardyce, B.; Shastri, Y.; Agrawal, R. Nanocellulose: Resources, physicochemical properties, current uses and future applications. *Front. Nanotechnol.* **2021**, *3*, 747329. [\[CrossRef\]](#)

25. Yadav, C.; Saini, A.; Zhang, W.; You, X.; Chauhan, I.; Mohanty, P.; Li, X. Plant-based nanocellulose: A review of routine and recent preparation methods with current progress in its applications as rheology modifier and 3D bioprinting. *Int. J. Biol. Macromol.* **2021**, *166*, 1586–1616. [[CrossRef](#)] [[PubMed](#)]
26. Khalil, H.A.; Davoudpour, Y.; Islam, M.N.; Mustapha, A.; Sudesh, K.; Dungani, R.; Jawaid, M. Production and modification of nanofibrillated cellulose using various mechanical processes: A review. *Carbohydr. Polym.* **2014**, *99*, 649–665. [[CrossRef](#)] [[PubMed](#)]
27. Ramesh, S.; Radhakrishnan, P. Cellulose nanoparticles from agro-industrial waste for the development of active packaging. *Appl. Surf. Sci.* **2019**, *484*, 1274–1281. [[CrossRef](#)]
28. Liu, X.; Sun, H.; Mu, T.; Fauconnier, M.L.; Li, M. Preparation of cellulose nanofibers from potato residues by ultrasonication combined with high-pressure homogenization. *Food Chem.* **2023**, *413*, 135675. [[CrossRef](#)]
29. Impoolsup, T.; Chiewchan, N.; Devahastin, S. On the use of microwave pretreatment to assist zero-waste chemical-free production process of nanofibrillated cellulose from lime residue. *Carbohydr. Polym.* **2020**, *230*, 115630. [[CrossRef](#)]
30. Sidana, A.; Yadav, S.K. Recent developments in lignocellulosic biomass pretreatment with a focus on eco-friendly, non-conventional methods. *J. Clean. Prod.* **2022**, *335*, 130286. [[CrossRef](#)]
31. Mankar, A.R.; Pandey, A.; Modak, A.; Pant, K. Pretreatment of lignocellulosic biomass: A review on recent advances. *Bioresour. Technol.* **2021**, *334*, 125235. [[CrossRef](#)] [[PubMed](#)]
32. Lobato-Peralta, D.R.; Duque-Brito, E.; Villafan-Vidales, H.I.; Longoria, A.; Sebastian, P.; Cuentas-Gallegos, A.K.; Arancibia-Bulnes, C.A.; Okoye, P.U. A review on trends in lignin extraction and valorization of lignocellulosic biomass for energy applications. *J. Clean. Prod.* **2021**, *293*, 126123. [[CrossRef](#)]
33. Saito, T.; Kimura, S.; Nishiyama, Y.; Isogai, A. Cellulose nanofibers prepared by TEMPO-mediated oxidation of native cellulose. *Biomacromolecules* **2007**, *8*, 2485–2491. [[CrossRef](#)] [[PubMed](#)]
34. Isogai, A.; Saito, T.; Fukuzumi, H. TEMPO-oxidized cellulose nanofibers. *Nanoscale* **2011**, *3*, 71–85. [[CrossRef](#)]
35. El-Sakhawy, M.; Kamel, S.; Salama, A.; Tohamy, H.-A.S. Preparation and infrared study of cellulose based amphiphilic materials. *Cellul. Chem. Technol.* **2018**, *52*, 193–200.
36. Jiang, J.; Wang, X. Adsorption of Hg (II) ions from aqueous solution by thiosemicarbazide-modified cellulose adsorbent. *BioResources* **2019**, *14*, 4670–4695. [[CrossRef](#)]
37. Harini, K.; Ramya, K.; Sukumar, M. Extraction of nano cellulose fibers from the banana peel and bract for production of acetyl and lauroyl cellulose. *Carbohydr. Polym.* **2018**, *201*, 329–339. [[CrossRef](#)]
38. Chowdhury, Z.Z.; Abd Hamid, S.B. Preparation and characterization of nanocrystalline cellulose using ultrasonication combined with a microwave-assisted pretreatment process. *BioResources* **2016**, *11*, 3397–3415. [[CrossRef](#)]
39. Hosseini, S.S.; Khodaiyan, F.; Yarmand, M.S. Optimization of microwave assisted extraction of pectin from sour orange peel and its physicochemical properties. *Carbohydr. Polym.* **2016**, *140*, 59–65. [[CrossRef](#)]
40. Gong, J.; Li, J.; Xu, J.; Xiang, Z.; Mo, L. Research on cellulose nanocrystals produced from cellulose sources with various polymorphs. *RSC Adv.* **2017**, *7*, 33486–33493. [[CrossRef](#)]
41. Xie, J.; Hse, C.-Y.; De Hoop, C.F.; Hu, T.; Qi, J.; Shupe, T.F. Isolation and characterization of cellulose nanofibers from bamboo using microwave liquefaction combined with chemical treatment and ultrasonication. *Carbohydr. Polym.* **2016**, *151*, 725–734. [[CrossRef](#)] [[PubMed](#)]
42. Kandhola, G.; Djiroleu, A.; Rajan, K.; Labbé, N.; Sakon, J.; Carrier, D.J.; Kim, J.-W. Maximizing production of cellulose nanocrystals and nanofibers from pre-extracted loblolly pine kraft pulp: A response surface approach. *Bioresour. Bioprocess.* **2020**, *7*, 1–16. [[CrossRef](#)]
43. Kasyapi, N.; Chaudhary, V.; Bhowmick, A.K. Bionanowhiskers from jute: Preparation and characterization. *Carbohydr. Polym.* **2013**, *92*, 1116–1123. [[CrossRef](#)] [[PubMed](#)]
44. Rajinipriya, M.; Nagalakshmaiah, M.; Robert, M.; Elkoun, S. Homogenous and transparent nanocellulosic films from carrot. *Ind. Crops Prod.* **2018**, *118*, 53–64. [[CrossRef](#)]
45. Dilamian, M.; Noroozi, B. A combined homogenization-high intensity ultrasonication process for individualization of cellulose micro-nano fibers from rice straw. *Cellulose* **2019**, *26*, 5831–5849. [[CrossRef](#)]
46. Hassan, M.L.; Mathew, A.P.; Hassan, E.A.; Oksman, K. Effect of pretreatment of bagasse pulp on properties of isolated nanofibers and nanopaper sheets. *Wood Fiber Sci.* **2010**, *42*, 362–376.
47. Kim, U.-J.; Kuga, S.; Wada, M.; Okano, T.; Kondo, T. Periodate oxidation of crystalline cellulose. *Biomacromolecules* **2000**, *1*, 488–492. [[CrossRef](#)]
48. Nair, S.S.; Zhu, J.; Deng, Y.; Ragauskas, A.J. Characterization of cellulose nanofibrillation by micro grinding. *J. Nanoparticle Res.* **2014**, *16*, 2349. [[CrossRef](#)]
49. Zhang, B.; Huang, C.; Zhao, H.; Wang, J.; Yin, C.; Zhang, L.; Zhao, Y. Effects of cellulose nanocrystals and cellulose nanofibers on the structure and properties of polyhydroxybutyrate nanocomposites. *Polymers* **2019**, *11*, 2063. [[CrossRef](#)]
50. González, K.; Retegi, A.; González, A.; Eceiza, A.; Gabilondo, N. Starch and cellulose nanocrystals together into thermoplastic starch bionanocomposites. *Carbohydr. Polym.* **2015**, *117*, 83–90. [[CrossRef](#)]
51. Mandal, A.; Chakrabarty, D. Isolation of nanocellulose from waste sugarcane bagasse (SCB) and its characterization. *Carbohydr. Polym.* **2011**, *86*, 1291–1299. [[CrossRef](#)]
52. Kumar, A.; Negi, Y.S.; Choudhary, V.; Bhardwaj, N.K. Characterization of cellulose nanocrystals produced by acid-hydrolysis from sugarcane bagasse as agro-waste. *J. Mater. Phys. Chem.* **2014**, *2*, 1–8. [[CrossRef](#)]

53. Soni, B.; Mahmoud, B. Chemical isolation and characterization of different cellulose nanofibers from cotton stalks. *Carbohydr. Polym.* **2015**, *134*, 581–589. [[CrossRef](#)]
54. Pacaphol, K.; Aht-Ong, D. Preparation of hemp nanofibers from agricultural waste by mechanical defibrillation in water. *J. Clean. Prod.* **2017**, *142*, 1283–1295. [[CrossRef](#)]
55. Masruchin, N.; Kurniawan, Y.; Kusumah, S.; Amanda, P.; Suryanegara, L.; Nuryawan, A. TEMPO-mediated oxidation cellulose pulp modified with Monosodium Glutamate (MSG). *Proc. IOP Conf. Ser. Earth Environ. Sci.* **2019**, *374*, 012010. [[CrossRef](#)]
56. Rohaizu, R.; Wanrosli, W. Sono-assisted TEMPO oxidation of oil palm lignocellulosic biomass for isolation of nanocrystalline cellulose. *Ultrason. Sonochemistry* **2017**, *34*, 631–639. [[CrossRef](#)] [[PubMed](#)]
57. Yamato, K.; Yoshida, Y.; Kumamoto, Y.; Isogai, A. Surface modification of TEMPO-oxidized cellulose nanofibers, and properties of their acrylate and epoxy resin composite films. *Cellulose* **2022**, *29*, 2839–2853. [[CrossRef](#)]

**Disclaimer/Publisher's Note:** The statements, opinions and data contained in all publications are solely those of the individual author(s) and contributor(s) and not of MDPI and/or the editor(s). MDPI and/or the editor(s) disclaim responsibility for any injury to people or property resulting from any ideas, methods, instructions or products referred to in the content.